APPLICATION OF THE HYBRID FINITE ELEMENT MIXING CELL METHOD TO AN ABANDONED COALFIELD IN BELGIUM

S. Wildemeersch[1, 2], S. Brouyère[1], Ph. Orban[1], J. Couturier[1], C. Dingelstadt[3], M. Veschkens[3], and A. Dassargues[1]

[1]University of Liege, ArGEnCo, GEO³; Hydrogeology and Environmental Geology, Aquapôle, B52/3 Sart-Tilman, 4000 Liege, Belgium

[2]F.R.I.A. - F.R.S.-FNRS - 1000 Brussels, Belgium

[3]ISSeP - Rue du Chéra 200, 4000 Liege, Belgium

Corresponding author : Wildemeersch Samuel

Address: University of Liege, ArGEnCo, GEO³; Hydrogeology and Environmental Geology, Aquapôle, B52/3 Sart-Tilman, 4000 Liege, Belgium

E-mail (work): swildemeersch@ulg.ac.be

Phone number (work): +32(0)43669553

Fax number (work): +32(0)43669520

Abstract

The Hybrid Finite Element Mixing Cell (HFEMC) method is a flexible modelling technique particularly suited to mining problems. The principle of this method is to subdivide the modelled zone into several subdomains and to select a specific equation, ranging from the simple linear reservoir equation to the groundwater flow in porous media equation, to model groundwater flow in each subdomain. The model can be run in transient conditions, which makes it a useful tool for managing mine closure post-issues such as groundwater rebound and water inrushes.

The application of the HFEMC method to an abandoned underground coal mine near the city of Liege (Belgium) is presented. The case study zone has been discretized taking advantage of the flexibility of the method. Then, the model has been calibrated in transient conditions based on both hydraulic head and water discharge rate observation and an uncertainty analysis has been performed. Finally, the calibrated model has been used to run several scenarios in order to assess the impacts of possible future phenomena on the hydraulic heads and the water discharge rates. Among others, the simulation of an intense rainfall event shows a quick and strong increase in hydraulic heads in some zones coupled with an increase in associated water discharge rates. This could lead to stability problems in local hill slopes. These predictions will help managing and predicting mine water problems in this complex mining system.

Keywords: Groundwater model; Mining works; HFEMC method; SUFT3D.

1 INTRODUCTION

Groundwater flow modelling in mined ground is challenging. Classical modelling techniques solving the flow in porous media equation fail to simulate groundwater flow in large voids constituting preferential flowpaths (Sherwood and Younger 1994; Sherwood and Younger, 1997; Younger et al., 2002; Rapantova et al., 2007). Another limitation on the use of classical modelling techniques in mined areas is related to the lack of knowledge of the hydrogeological conditions and to the scarcity of data concerning the mine workings and their possible interconnections. Consequently, specific implicit and explicit modelling techniques have been developed for mined areas. These techniques range from box model techniques (Sherwood and Younger, 1997) to physically-based and spatially-distributed techniques (Adams and

Younger, 1997; Younger et al., 2002; Boyaud and Therrien, 2004), including the new HFEMC method (Brouyère et al., 2009).

The HFEMC method couples groups of mixing cells for the mine workings with finite elements for the unmined zone. The interactions between the mined zones and the unmined zone are considered using internal boundary conditions which are defined at the interfaces between the groups of mixing cells and the finite element mesh. Another feature of this technique lies in its ability to simulate by-pass flows between mine workings using first order transfer equations between the groups of mixing cells. The HFEMC method is particularly useful to simulate mine groundwater problems such as groundwater rebound. This kind of phenomenon is essential to simulate since consequences such as soil instability, flooding, and water inrushes can be harmful (Younger et al., 2002).

The first application of the HFEMC method focuses on an abandoned underground coal mine near the city of Liege (Belgium). The conceptual model and the calibration in steady-state conditions have already been presented (Brouyère et al., 2009). The main goal of this paper is to show the capacity of the HFEMC method to model groundwater and mine water flows in transient conditions and for the simulation of the mined water system responses to different extreme hydrological scenarios. This paper presents the calibration in transient conditions, the scenarios simulations performed with the calibrated model, and the conclusions and the perspectives of this first application in transient conditions of the HFEMC method.

2 FUNDAMENTAL PRINCIPLE OF THE HFEMC METHOD

A full presentation of the HFEMC method, including verification and illustration test cases, was presented by Brouyère et al. (2009). The fundamental principle of the technique is to subdivide the modelled zone into mined and unmined zones. The mining works are discretised by groups of mixing cells and modelled using linear reservoirs characterised by a mean water level (Eq. 1a). The unmined zone is discretised by finite elements providing spatially-distributed hydraulic heads obtained through the finite element solution of the groundwater flow equation in porous media (Eq. 1b). Choosing different equations for the mined zones and the unmined zone reflects the different level of knowledge of hydrogeological conditions in each of them. The mining works are often poorly hydrogeologically characterised compared with the unmined zone. Furthermore, the groundwater flow in porous media equation is not valid in the large voids of the mining works.

$$Q_{LR} = S_{LR}\ A_{LR,upper} \frac{\partial H_{LR}}{\partial t} = -\alpha_{LR}\ A_{LR,exc} \left(H_{LR} - H_{ref}\right) + Q \qquad (1a)$$

$$F \frac{\partial h}{\partial t} = \underline{\nabla}\left(\underline{\underline{K}}\, \underline{\nabla}\left(h + z\right)\right) + q \qquad (1b)$$

where Q_{LR} = flow rate entering or leaving the linear reservoir [L^3T^{-1}], S_{LR} = storage of the linear reservoir [-], $A_{LR,upper}$ = area of the upper face of the linear reservoir [L^2], H_{LR} = mean hydraulic head in the linear reservoir [L], α_{LR} = exchange coefficient of the linear reservoir [T^{-1}], $A_{LR,exc}$ = area of the exchange face of the linear reservoir [L^2], H_{ref} = drainage level of the linear reservoir [L], Q = source/sink term [L^3T^{-1}], F = specific storage coefficient of the porous medium [L^{-1}], h = pressure potential [L], $\underline{\underline{K}}$ = hydraulic conductivity tensor [LT^{-1}], z = gravity potential [L], and q = source/sink term by unit volume [T^{-1}].

The interactions between mined and unmined zones are considered via internal boundary conditions defined at the interfaces between the groups of mixing cells and the finite elements. Three types of internal boundary are available: Dirichlet (first-type) *dynamic* boundary condition (Eq. 2a), Neumann (second-type) *impervious* boundary condition (2b), and Fourier (third-type) *dynamic* boundary condition (2c). The term *dynamic* is used for underlining the fact that the hydraulic heads used in these boundary conditions are variable with time and the remaining unknowns within the problem.

$$h_{SD,i}(x,y,z,t) = h_{SD,j}(x,y,z,t) \qquad (2a)$$

$$\frac{h(x,y,z,t)}{\partial n} = 0 \qquad (2b)$$

$$Q_{SD,i-SD,j} = \alpha_{FBC}\ A_{exc}\left(h_{SD,j}(x,y,z,t) - h_{SD,i}(x,y,z,t)\right) \qquad (2c)$$

where $h_{SD,i}$ = the hydraulic head in sub-domain *i* [L], $h_{SD,j}$ = the hydraulic head in sub-domain *j* [L], $Q_{SD,i-SD,j}$ = exchanged flow between sub-domains *i* and *j* through the third-type of *internal* boundary condition [L^3T^{-1}], α_{FBC} = exchange coefficient for the third type of *internal* boundary condition [T^{-1}], and A_{exc} = the exchange area for the third type of *internal* boundary condition [L^2].

The term α_{FBC} is a function of the hydraulic conductivity on both sides of the interface between interacting subdomains. This term is estimated during the calibration process.

The interactions between the mining works themselves, that is by-pass flow connections through old mine workings such as shafts or galleries, are modelled using a first-order transfer equation (Eq. 3). These by-pass flow connections can be switched on and off to simulate water inrushes.

$$Q_{SD,i-SD,j} = \alpha_{BF} \left(h_{SD,j}(x,y,z,t) - h_{SD,i}(x,y,z,t)\right) \quad (3)$$

The exchange coefficient α_{BF} (L^2T^{-1}) is related to the head losses along preferential flow paths.

A general schema of the HFEMC method is proposed in Figure 1.

3 CASE STUDY: AN ABANDONED UNDERGROUND COAL MINE IN BELGIUM

The abandoned underground coal mine of Cheratte is located downstream of the city of Liege (Belgium) (Figure 2). The zone of interest covers about 27 km². The altitude ranges from about 55 m in the alluvial plain of the Meuse River to 200 m on the plateau. The rivers crossing the zone are the Meuse River and three of its direct or indirect tributaries flowing mainly northward (Figure 3).

The Cheratte underground coal mine comprising mined zones, *Trembleur*, *Argenteau*, *Hasard-Cheratte Nord*, *Hasard-Cheratte Sud*, and *Wandre*, each made up of a network of galleries (Figure 3). These mined zones interact with the surface water network and with the surrounding unmined zone.

The mined zones are located in a faulted and folded geological formation comprising shales and silts with intercalations of sandstones, quartzites, and coal seams (Houiller Group - HOU - Upper Carboniferous).

The overlying geological formations comprise clays and sands (Vaals formation - VAA - Cretaceous), chalk (Gulpen formation - GUL - Cretaceous), clays, silts and sands (terraces of the Meuse River - ALA - Tertiary), pebbles, sands and clays (alluvial deposits of the Meuse River - AMO - Quaternary) (Barchy and Marion, 2000) (Figure 3).

The main aquifer of the case study zone is located in the chalk of the Gulpen formation. The groundwater is influenced by both the dip of the Cretaceous formations and the Meuse River, and flows mainly towards the northwest. However, this general trend is disturbed in the vicinity of the mined zones where significant drawdowns are observed. As indicated by the strong correlation observed between hydraulic heads and water discharge rates (Figure 4). Some of these mined zones are probably connected through faults and unlisted mine workings. As an example, the water discharge rate in the drainage gallery of *Hasard-Cheratte Sud* (E8) correlates closely with the hydraulic heads in *Argenteau* (Pz4) and *Trembleur* (Pz7) although the hydraulic head in *Hasard-Cheratte Sud* (Pz8) is almost stable. Connections must exist between *Hasard-Cheratte Sud* and both *Argenteau* and *Trembleur*. The hydraulic head thresholds from which the groundwater within *Argenteau* and *Trembleur* is evacuated directly through the drainage gallery of *Hasard-Cheratte Sud* are estimated at 88.5 m and 102 m above mean sea level (amsl), respectively (Dingelstadt et al., 2007).

Cheratte underground coal mine was closed in the end of the 1970s. The last pumping, maintaining the groundwater level in *Trembleur* at about -64 m amsl ceased in 1982. However, the groundwater rebound was not recorded until the installation of a monitoring network in 2003. Water levels and water discharge rate measurements are now recorded regularly in a series of piezometers and drainage galleries (Figure 3). Although trend analysis from such a time series is difficult, the groundwater rebound still seems to be ongoing from the hydraulic head trends in *Argenteau* (Pz4) and *Trembleur* (Pz7). However, most of the groundwater rebound has probably already taken place.

4 GROUNDWATER FLOW MODELLING OF THE CHERATTE UNDERGROUND COAL MINE

4.1 Conceptual and numerical models

A Fourier (third-type) boundary condition is prescribed at the western external boundary of the model to consider the exchange of water between the aquifer and the Meuse River. A Neumann (second-type) impervious boundary condition is prescribed at the northern, eastern and southern external boundaries assuming they correspond to groundwater divides or faults filled with clay. Based on a groundwater budget (Dingelstadt et al., 2007), a recharge is assigned on the top of the model. The top of the model corresponds to the topography and the base of the model is the -64 m amsl plane. The corresponding mesh is composed of 3 layers, 30,443 nodes, and 40,976 elements.

The model is subdivided into eight subdomains: five corresponding to the mined zones of *Trembleur*, *Argenteau*, *Hasard-Cheratte Nord*, *Hasard-Cheratte Sud*, and *Wandre*, two corresponding to mine water collecting pipes, and one corresponding to the adjacent and overlying unmined zone. The internal boundary conditions between mined zones and unmined zones are defined as Fourier (third-type) *dynamic* boundary conditions in order to allow groundwater flux exchanges. Ten by-pass flow connections between mined zones are considered. The identification and the adjustment of these by-pass flow connections are based on previous results obtained with a box model calibrated in steady-state conditions using EPANET 2.0 (Rossman, 2000; Gardin et al., 2005) as well as on the correlation observed between hydraulic heads and water discharge rate measurements performed in the mined zones (Figure 4). The hydraulic head thresholds highlighted by these measurements are also taken into account. Consequently, the connections *Argenteau* ↔ *Hasard-Cheratte Sud* and *Trembleur* ↔ *Hasard-Cheratte Sud* are switched on only when hydraulic heads in *Argenteau* and *Trembleur* are higher than 88.5 m and 102 m amsl, respectively. Additional information concerning the conceptual model can be found in Brouyère et al. (2009).

4.2 Calibration in transient conditions

The calibration in transient conditions is based on both hydraulic head and water discharge rate observations performed from January 2004 to December 2005. The initial conditions for the calibration in transient conditions derive from calibration under steady-state condition (Brouyère et al., 2009). As suggested by Hill and Tiedeman (2007) and since the prescribed recharge varies monthly (only available data), the observations are monthly averaged to ensure time-consistency between observed and simulated values. The calibrated parameters are given by the hydraulic conductivities of the geological formations, the exchange coefficients of both internal and external Fourier boundary conditions, and the exchange coefficients of by-pass flow connections between mined zones and also the specific yield and the specific storage coefficients of both mined zones and geological formations of the unmined zones. The list of parameters used for these transient simulations is given in Table 1. Graphic comparisons between observed and simulated values in terms of hydraulic heads and water discharge rates are presented in Figure 5 and Figure 6, respectively.

The calibrated model reproduces the observed hydraulic heads with a range of error up to 10 m and water discharge rates with a range of error up to 10L /s. These are directly related to the simulated hydraulic heads since they are represented by Fourier boundary conditions or by by-pass flow connections for which computed flow rates depend on the difference between hydraulic heads. The simulated water discharge rate and hydraulic head in *Argenteau* (E2 and Pz4) are similar. The situation is more complex for *Hasard-Cheratte Sud* (E8 and Pz8) since the simulated water discharge rate of this mined zone is also related to the hydraulic heads in *Argenteau* (Pz4) and *Trembleur* (Pz7). Observations indicate that the hydraulic head thresholds of *Argenteau* (88.5 m) and *Trembleur* (102 m) were exceeded from February 2005 to June 2005 with a major peak in February and a minor peak in May. Accordingly, two flooding peaks are observed in the drainage gallery of *Hasard-Cheratte Sud*. The simulated hydraulic heads reproduce the major peaks observed but not the minor ones probably because of recharge which is based on monthly effective rainfall. The simulated water discharge rate consequently reproduces only the first flooding peak.

4.3 Analysis of sensitivity and uncertainty

A sensitivity and uncertainty analysis is performed using UCODE_2005 (Poeter et al., 2005). The sensitivity analysis is performed for the period January 2004-March 2004 with 38 hydraulic head observations and 22 parameters using their calibrated values. The sensitivities of the hydraulic conductivity and specific yield of geological formations are evaluated using multipliers. As suggested by

Hill and Tiedeman (2007), a weight of 0.44 m^{-2} (inverse of the variance) is assigned to all hydraulic head observations, assuming a standard deviation of the errors in hydraulic head observations of 1.5 m. The observation error includes error on the elevation and water depth measurements and errors linked to the mesh whose nodes do not correspond exactly to the observation points. Consequently, comparison between observed and simulated values is performed using the closest node to the observation point sometimes located several tens of meters away. Considering these three sources of error, a mean observation error of 1.5 m is reasonable.

The most useful statistic provided by UCODE_2005 for estimating the global sensitivity of a parameter is the composite scaled sensitivity (css) (Eq. 4) (Hill, 1992; Anderman et al., 1996; Hill et al., 1998; Hill and Tiedeman, 2007). This statistic is a measure of the sensitivity of one parameter to all the observations. A parameter with a css value less than 1.00 or less than 1/100 of the maximum css value is considered as poorly sensitive (Hill and Tiedeman, 2007). The css values obtained for each parameter are listed in Table 2.

$$css_j = \left[\sum_{i=1}^{ND} (dss_{ij})^2 \Big|_{\underline{b}} / ND \right]^{1/2} \text{ with } dss_{ij} = \left(\frac{\partial y_i'}{\partial b_j} \right) \Big|_{\underline{b}} \left| b_j \right| \omega_{ii}^{1/2} \quad (4)$$

where dss_{ij}=*dimensionless scaled sensitivity* of the simulated value associated to the *i*th observation with respect to the *j*th parameter, $\left(\frac{\partial y_i'}{\partial b_j} \right)$=sensitivity of the simulated value associated with the *i*th observation with respect to the *j*th parameter evaluated at the set of parameter values in *b*, b_j=*j*th parameter, ω_{ii} =the weight of the *i*th observation, and *ND*=number of observations.

The most sensitive parameters are K, S_y, S_y - *Trembleur*, and α - *Argenteau* - Meuse R. These parameters are related to the storage of the geological formations and to the storage and the drainage of the largest mined zones (*Trembleur* and *Argenteau*) showing their influence on the model and, therefore, on the groundwater flow of the case study zone. The other parameters are relatively insensitive to the hydraulic head observations.

The uncertainty analysis is performed for the period September 2004-Augustus 2005 using the parameters with a high composite scaled sensitiviy (css) and relatively high prediction scaled sensitivity (pss) (Eq. 5).

This latter statistic indicates the importance of the parameter values to the predictions (Hill and Tiedeman, 2007).

$$pss_{lj} = \left(\frac{\partial z_l^{'}}{\partial b_j}\right)\left(\frac{b_j}{100}\right)\left(\frac{100}{z_l^{'}}\right) \quad (5)$$

where $\left(\frac{\partial z_l^{'}}{\partial b_j}\right)$=sensitivity of the simulated value associated with the *l*th prediciton with respect to the *j*th parameter, b_j=*j*th parameter.

The parameters used are K, S_y, S_y - *Trembleur*, α - *Argenteau* - Meuse R, S_y - *Argenteau*, $\alpha_{\textit{Trembleur-Hasard-Cheratte Nord}}$, and $\alpha_{\textit{Hasard-Cheratte Nord}\text{-collecting pipe 2}}$. Parameters characterised by a small pss are not included in the uncertainty analysis since they are not important for the predictions of interest (Hill and Tiedeman, 2007). Linear individual confidence intervals with a level of confidence of 5% are calculated for 3 observations points: Pz7 - *Trembleur* (mine workings with high annual hydraulic head variations), F5 - *Wandre* (mine workings with small annual hydraulic head variations) and F8 (unmined zone) (Figure 7).

Confidence intervals are relatively small for F5 and F8 while confidence interval for Pz7 is larger. This is probably related to the uncertainty about the parameters $\alpha_{\textit{Trembleur-Hasard-Cheratte Nord}}$ and $\alpha_{\textit{Hasard-Cheratte Nord}\text{-collecting pipe 2}}$. On the one hand, these parameters have a css > 1.00 (respectively 7.71 x 10^{-1} and 3.31 x 10^{-1}) meaning that they are relatively imprecise. On the other hand, they have a relatively large pss meaning that they are relatively important to the predictions of interest. As suggested by Hill and Tiedeman (2007), improving the estimation of these parameters could reduce the confidence intervals on the predictions. However, the main objective of this paper is to show the capacity of the HFEMC method in mined ground and transient conditions rather than extreme calibration of the model.

4.4 Groundwater rebound, water inrush, and wet winter scenarios

The goal of the scenarios is to support the managment of the abandoned underground coal mine of Cheratte by simulating system response to extreme conditions.

4.4.1 Groundwater rebound

According to the hydraulic heads measured since 2003, much of the Cheratte underground coal mine groundwater rebound has probably already taken place. The aim of this scenario is to try to reproduce this past event for confirming this hypothesis.

The only data available concerning dewatering operations indicates that the last pumping phase was stopped in 1982. Previously, pumping maintained the water level at -64 m amsl in *Trembleur*. A thirty years simulation is performed for simulating the period 1977-2007. The first part of the simulation (5 years) is performed with a sink term withdrawing about 5000 m³/day in *Trembleur*. As no data concerning the pumping rates were available, a value of 5000 m³/day was obtained by trial and error until the water level in *Trembleur* reaches -64 m amsl. The second part (25 years) of the simulation was performed without any pumping. A constant recharge of 189 mm/year, equivalent to the mean annual recharge between 2003 and 2006, is prescribed during the whole simulation (30 years). The simulated hydraulic heads, the water discharge rates between mined zones, and the water discharge rates between mined zones and the surface waters are presented in Figure 8, and Figure 9, respectively. A negative water discharge rate means that the water flows from the first mined zone to the second mined zone.

As expected, the water level in *Trembleur* is -64 m amsl during the first five years of the simulation. Through their connections with *Trembleur*, the water levels in the other mined zones are also lowered. As highlighted by the exchanged flow rates between mined zones, *Argenteau* and *Hasard-Cheratte Nord* are the main mined zones which feed *Trembleur* during this period. The exchanged flow rates between the other mined zones are limited because of their low exchange coefficients (Table 1). There is no exchanged flow rate between *Argenteau* and *Hasard-Cheratte Sud* and between *Trembleur* and *Hasard-Cheratte Sud* because the water levels are lower than the respective thresholds of 88.5 m and 102 m. The mined zones are also fed by the Meuse River since the river stage is higher than groundwater levels nearby.

As soon as pumping phase in *Trembleur* was stopped, groundwater rebound took place until the system reached equilibrium. The simulation indicates that the exchanged flow rates reversed after two years and that most of the groundwater rebound (97 %) had occurred after about five years.

4.4.2 Water inrush

Groundwater rebound can induce harmful phenomena such as water inrushes which occur when a drainage gallery is obstructed. This causes a water level increase behind the obstruction until it breaks under pressure. The objective of this scenario is to predict the evolution of hydraulic heads and water discharge rates in the event of a water inrush in the gallery draining *Hasard-Cheratte Sud*.

The scenario simulates a period of two years with a prescribed recharge identical to that used in the calibration. Assuming a rock collapse at the end of the first month and an obstruction strength of 72.5 m amsl, the exchange coefficient between *Hasard-Cheratte Sud* and the collecting pipe 1 ($\alpha_{\textit{Hasard-Cheratte Sud-}\text{collecting pipe 1}}$) is set to 0 from the end of the first month until the hydraulic head in *Hasard-Cheratte Sud* reaches a value of 72.5 m amsl. The simulated hydraulic heads in some piezometers and the simulated water discharge rate are shown in Figure 10 and Figure 11, respectively.

The simulated hydraulic heads indicate an immediate though relatively slow water level increase in *Hasard-Cheratte Sud* from the obstruction of its drainage gallery until it breaks under a hydraulic head of 72.5 m. The other zones (mined or unmined) do not show any particular responses to this event. The simulated water level discharge rate in E8 is not only fed by *Hasard-Cheratte Sud* but also by *Trembleur* and *Argenteau* once their respective hydraulic head thresholds of 102 m amsl and 88.5 m amsl are exceeded. Consequently, even when the drainage gallery of *Hasard-Cheratte Sud* is obstructed, discharge can still occur in E8. This is what happens intermittently during the obstruction period. However, the water inrush is obvious since the water discharge rate in E8 increases instantaneously to about 9 L/s as soon as the obstruction breaks. After this event, the water discharge rate in E8 decreases slowly, following the slow water level decrease in *Hasard-Cheratte Sud*. The other drainage galleries do not show any particular responses. It is obvious that the intensity of the water inrush depends on the strength of the obstruction which has been set arbitrarily to 72.5 m in this scenario. Higher obstruction strength would have caused a stronger water inrush and vice versa.

4.4.3 Wet winter

Hydraulic head variations and water discharges observed since 2003 indicate that the mined zones react intensively and very quickly to strong rainfall events. The goal of this scenario is to predict the system response to a particularly wet winter.

The scenario simulates a period of three years with a very rainy winter at the end of the first year of simulation. The prescribed recharge varies monthly. Except for the period of the wet winter, the recharge rate is deduced from water balances computed between 2004 and 2006. The recharge prescribed for simulating the very rainy winter is 76 mm in December, 122 m in January, and 46 mm in February (about three times more than during an average winter). The simulated hydraulic heads in some piezometers and the simulated water discharge rate are shown in Figure 12 and Figure 13, respectively.

The mined zones are more influenced by a strong rainfall event than the unmined zone. It is particularly the case for *Argenteau* and *Trembleur* since their water levels increase by about 25 m in only three months. About six months are required afterwards to return to a normal situation. The simulated water discharge rate in E2 indicates an increase of about 15 l/s in three months. The maximum computed water discharge rate is about 30 l/s. Once more, about six months are then necessary to return to a normal situation. The simulated water discharge rate in E8 is more complex since it is related to the hydraulic head thresholds of both *Argenteau* (88.5 m) and *Trembleur* (102 m). These thresholds are reached almost at the same time and they cause an almost instantaneous increase of water discharge rate of about 15 l/s. Then, the water discharge continues to increase proportionally to the simulated hydraulic heads in *Argenteau* and *Trembleur* and finally reaches a value of about 30 l/s. As long as the simulated hydraulic heads in *Argenteau* and *Trembleur* are higher than the respective thresholds, the simulated water discharge rate in E8 remains high. Consequently, the simulated water discharge rate is between 20 l/s and 30 l/s for about six months. As highlighted by both the simulated hydraulic heads and water discharge rates, the other mined zones react less to the rainy winter.

This scenario shows that a wet winter could cause a strong increase in water levels in *Trembleur* and *Argenteau*. As a consequence, the water discharge rate in E2 and E8 could increase and remain high several months. This scenario shows also that *Hasard-Cheratte Sud* is the most sensitive mined zone. However, the model does not take into account old dewatering galleries which would modify the hydrogeology of the zone of interest and thus the system response.

5 CONCLUSIONS AND PERSPECTIVES

The HFEMC method, developed by Brouyère et al. (2009), is a flexible modelling technique applied to mine water problems. Thanks to the dynamic coupling between mixing cells for the mined zones and classical finite elements for the unmined zone, the method is an efficient compromise between the simple box model techniques and the complex physically-based and spatially-distributed techniques. Furthermore, this method is able to take into account by-pass flow connections between mined zones. The first application of the HFEMC method on a real case, the abandoned underground coal mine of Cheratte, is encouraging. The model is calibrated in both steady-state and transient conditions based on both hydraulic heads and water discharge rates. Despite the complex connections existing between mined zones, sometimes depending on hydraulic head thresholds, the method is able to fairly reproduce the time variations observed in terms of both hydraulic heads and water discharge rates. The uncertainty analysis indicates that the confidence intervals on the predictions are relatively high for the mined zones with high hydraulic head variations during the year. These confidence intervals could be reduced by improving the estimation of the key parameters for the predictions highlighted by the sensitivity analysis (mainly $\alpha_{\textit{Trembleur-Hasard-Cheratte Nord}}$ and $\alpha_{\textit{Hasard-Cheratte Nord}\text{-collecting pipe 2}}$). However, the main objective of this paper is not to give highly precise predictions but rather to show the capability of the method in mined ground and in transient conditions. The calibrated model can be used to simulate groundwater rebound and the system responses to a water inrush and wet winter. The first scenario indicates that much of the groundwater rebound had probably taken place in about five years but that the whole process had lasted the first twelve years. The second scenario shows that an obstruction of the drainage gallery of *Hasard-Cheratte Sud* could cause an immediate, though slow, water level increase in this mined zone, followed by a water inrush once the obstruction breaks. The third scenario indicates that a wet winter could cause strong hydraulic head increases in the mined zones (particularly in *Argenteau* and *Trembleur*). Consequently, water discharge rates would strongly increase as well and it could take about six months to return to a normal situation.

As a new set of observations is now available, future works will consist of improving and updating the calibration in transient conditions for reducing the uncertainty about predictions. A reactive transport model will also be developed to be able to simulate acid mine drainage phenomena induced by groundwater rebound in a lot of old mines.

ACKNOWLEDGEMENTS

The authors thank the Walloon Region, which has financially supported this project, together with the “Institut Scientifique de Service Public” (ISSeP) and the “Association Intercommunale pour le Démergement et l’Epuration” (AIDE). Conceptual and numerical developments of the HFEMC approach have also been performed in the framework of the Interuniversity Attraction Pole TIMOTHY (IAP Research Project P6/13), which is funded by the Belgian Federal Science Policy Office (BELSPO) and the European Integrated Project AquaTerra (GOCE 505428) with funding from the Community's Sixth Framework Programme. The authors thank also the editor Geoff Syme, the reviewer Nick Robins and one anonymous reviewer for their constructive comments and suggestions that help improving greatly the paper.

REFERENCES

Adams R., and Younger P. L., 1997, Simulation of groundwater rebound in abandoned mines using physically based modelling approach, 6^{th} International Mine Water Association Congress, IRGO & IMWA, Bled, Slovenia.

Anderman E. R., Hill M. C., and Poeter E. P., 1996, Two-Dimensional Advective Transport in Ground-Water Flow Parameter Estimation, Ground Water, **74**(2):212-218.

Barchy L., and J.-M. Marion (2000), Carte géologique de Wallonie et notice explicative - Dalhem-Herve 42/3-4, Ministère de la Région Wallonne - Direction Générale des Ressources Naturelles et de l'Environnement, Namur.

Boyaud C. and R. Therrien, 2004, Numerical modelling of mine water rebound in Saizerais, northeastern France, 15^{th} International Conference on Computational Method in Water Resources, Elsevier Science, Amsterdam, The Netherlands.

Brouyère S., Orban Ph., Wildemeersch S., Couturier J., Gardin N., and A. Dassargues, 2009, The Hybrid Finite Element Mixing Cell Method: A New Flexible Method for Modelling Mine Ground Water Problems, *Mine Water and the Environment*, **28**(2), 102-114.

Dingelstadt C., Drevet J.-P.,Veschkens M., and Flamion B., 2007, Etude des conséquences de l'après-mine en particulier sur la gestion des eaux souterraines et des risques - Mission 2006, 67 pp, Institut Scientifique de Service Public, Liège.

Gardin N., Brouyère S., and Dassargues A., 2005, Modélisation de la remontée des niveaux piézométriques dans les massifs affectés par des travaux miniers dans l’ancien bassin charbonnier liégeois - Site pilote de Cheratte, 90 pp, Université de Liège, Liège

Hill M. C., 1992, A Computer Program (MODFLOWP) for Estimating Parameters of a Transient, Three-Dimensional, Ground-Water Flow Model Using Non-Linear Regression, U.S. Geological Survey Open-File Report 91-184.

Hill M. C., Cooley R. L., Pollock D. W., 1998, A Controlled Experiment in Ground-Water Flow Model Calibration Using Nonlinear Regression, *Ground Water*, **36**(3):520-535.

Hill, M. C., and C. R. Tiedeman, 2007, Effective Groundwater Model Calibration: With Analysis of Data, Sensitivities, Predictions, and Uncertainty, John Wiley & Sons, Inc., Hoboken (New Jersey).

Poeter E. P., Hill M. C., Banta E. R., Mehl S., and Christensen S., 2005, UCODE_2005 and Six Other Computer Codes for Universal Sensitivity Analysis, Calibration, and Uncertainty Evaluation, U.S. Geological Survey Techniques and Methods TM 6-A11.

Rapantova N., Grmela A., Vojtek D., Halir J., and Michalek B., 2007, Ground water flow modelling applications in mining hydrogeology, *Mine Water and the Environment*, **26**, p. 264 - 270.

Rossman L. A., 2000, EPANET 2 - users manual, National Risk Management Research Laboratory, Office Of Research And Development, U.S. Environmental Protection Agency, Cincinnati, OH, 45268

Sherwood, J. M., and P. L. Younger, 1994, Modelling groundwater rebound after coalfield closure: an example from County Durham, 5th International Mine Water Association Congress, University of Nottingham and IMWA, University of Nottingham, United Kingdom.

Sherwood J. M., and Younger P. L., 1997, Modelling groundwater rebound after coalfield closure, Congress of the International Association of Hydrogeologists - Groundwater in the urban environment: Processes and Management.

Younger P. L., Banwart S. A., and Hedin S. H., 2002, Mine Water: Hydrology, Pollution, Remediation, Kluwer Academic Publishers.

Figure captions

Figure 1. General schema of the HFEMC method

Figure 2. Location of the case study zone

Figure 3. Geological map of the case study zone pointing out the mined zones (adapted from Barchy and Marion (2000))

Figure 4. Correlation between observed hydraulic heads and observed water discharge rates (adapted from Dingelstadt et al. (2007))

Figure 5. Comparison between observed and simulated hydraulic heads in different piezometers of the case study zone

Figure 6. Comparison between observed and simulated water discharge rates

Figure 7. 95% linear individual confidence intervals for observation points Pz7, F5, and F8

Figure 8. Groundwater rebound scenario - Simulated hydraulic heads

Figure 9. Groundwater rebound scenario - (A) Simulated water discharge rates between mined zones and (B) Simulated water discharge rates between mined zones and the surface waters

Figure 10. Water inrush scenario - Simulated hydraulic heads in different piezometers of the case study zone

Figure 11. Water inrush scenario - Simulated water discharge rates

Figure 12. Wet winter scenario - Simulated hydraulic heads in different piezometers of the case study zone

Figure 13. Wet winter scenario - Simulated water discharge rates

Table captions

Table 1. Calibrated parameters in transient conditions

Table 2. Composite scaled sensitivity (css) computed by UCODE_2005 using calibrated parameter values and a total of 38 hydraulic head observations.

Figure 1
Click here to download high resolution image

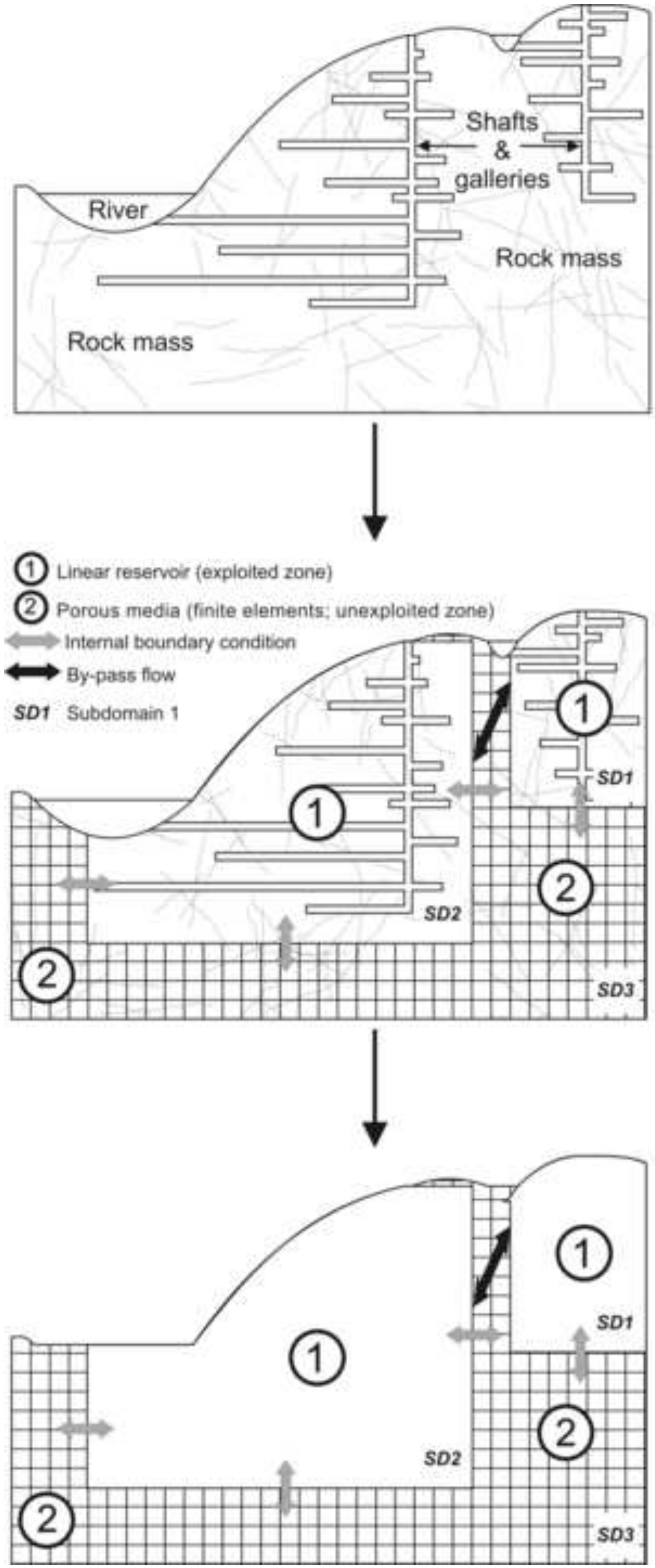

Figure 2
Click here to download high resolution image

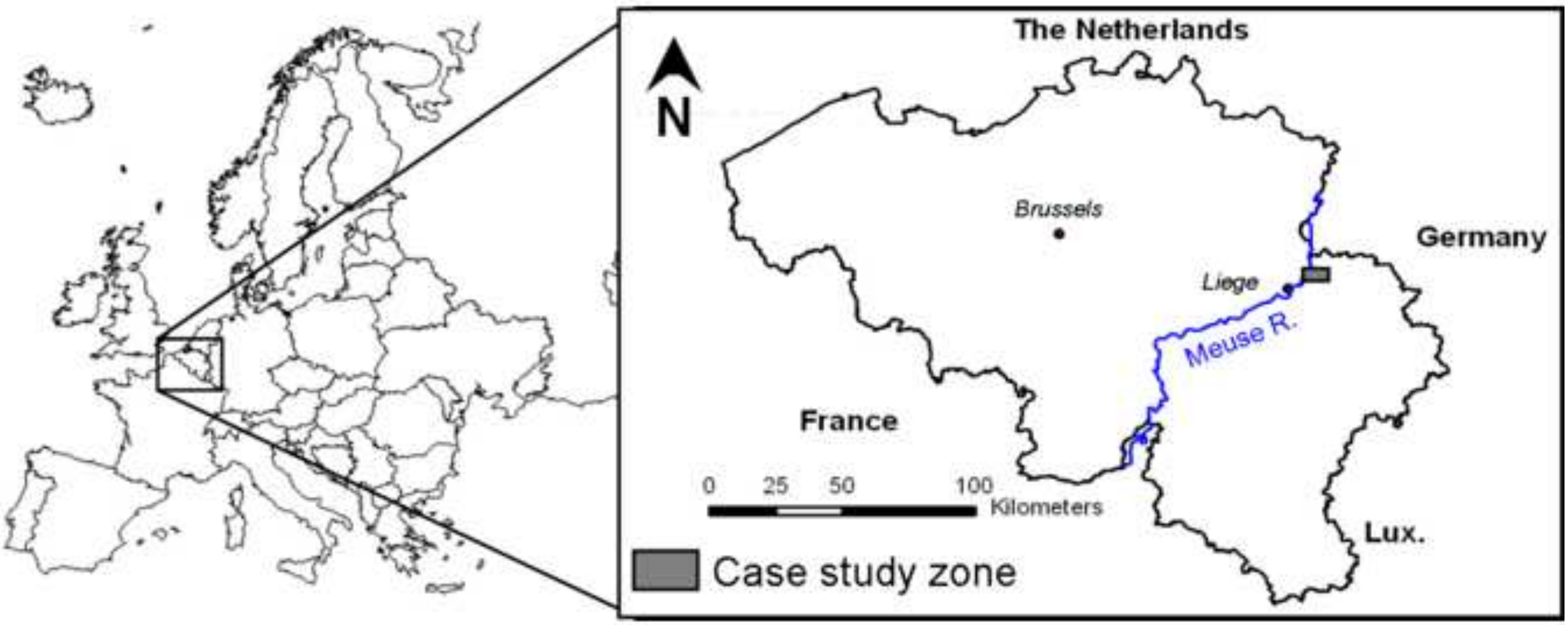

Figure 3
Click here to download high resolution image

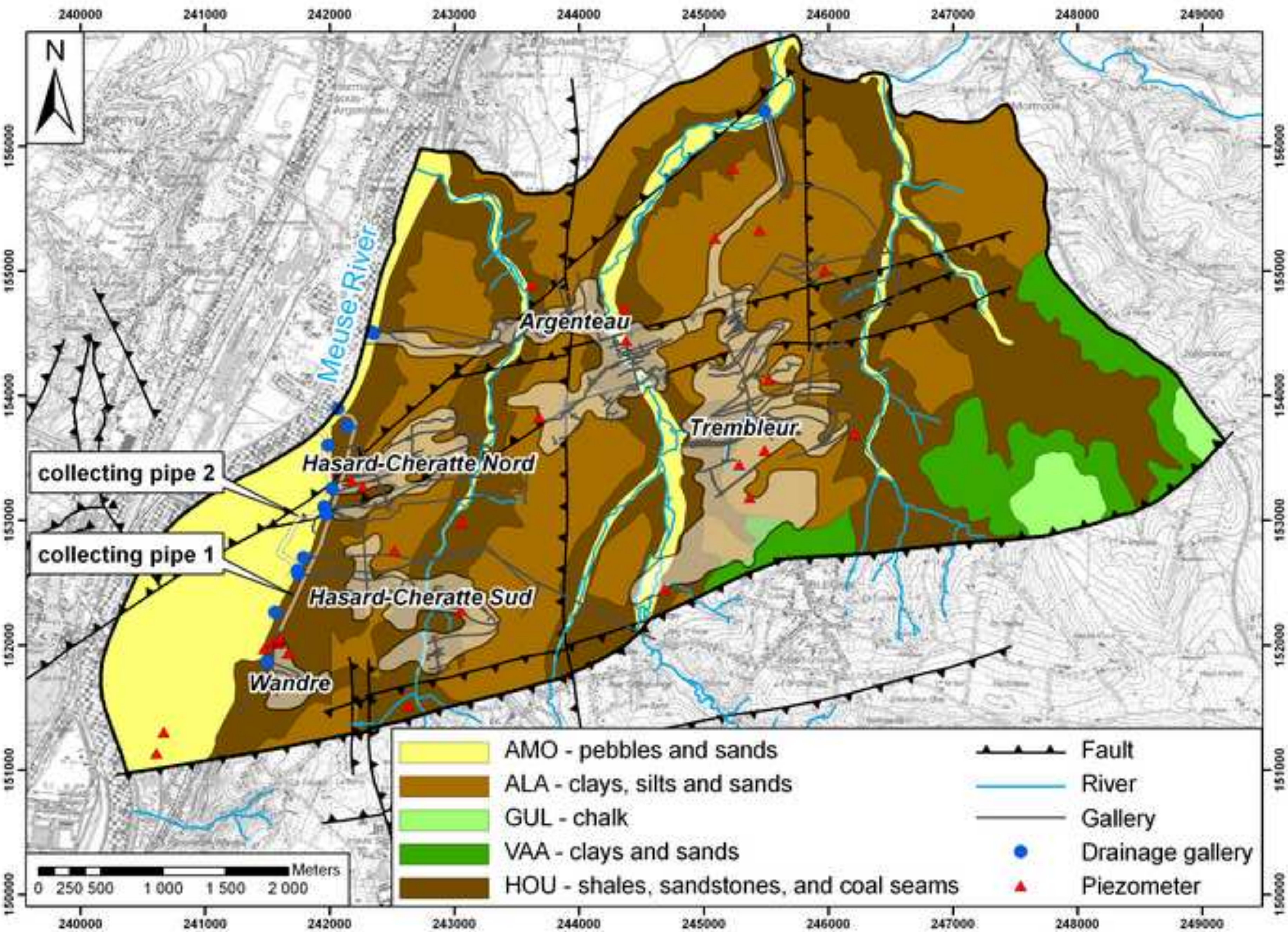

Figure 4

Click here to download high resolution image

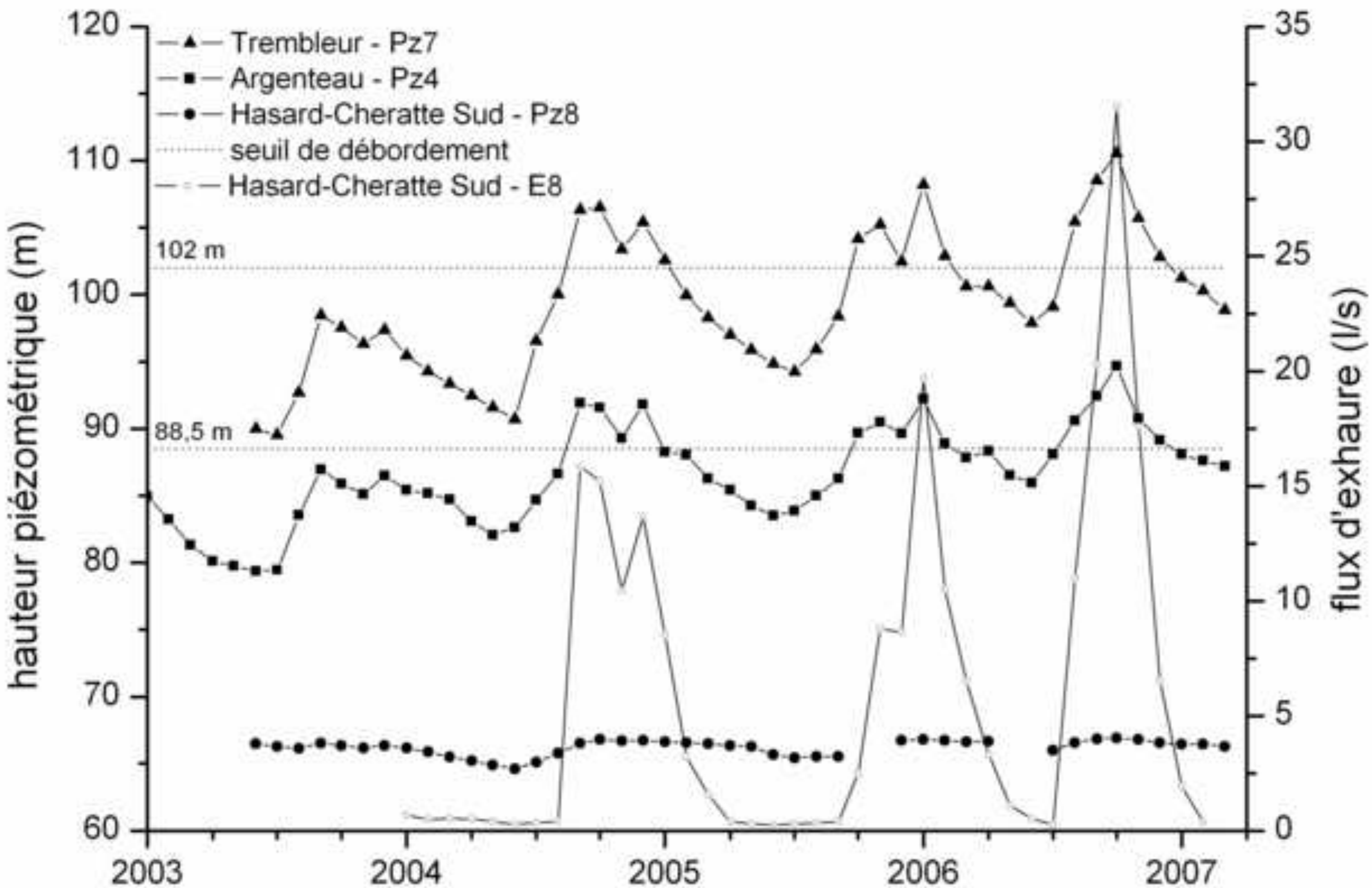

Figure 5

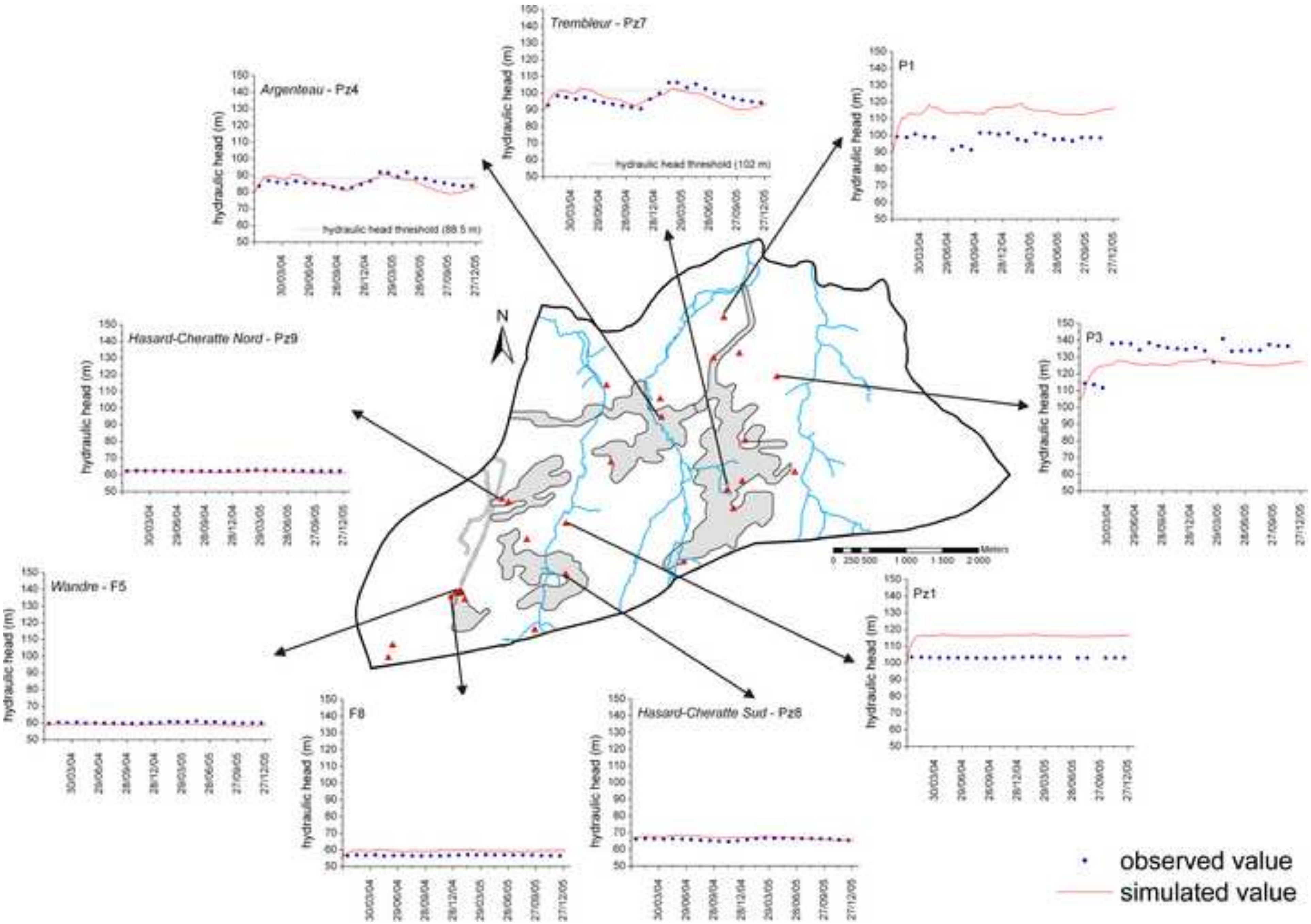
Argenteau - Pz4
hydraulic head threshold (88.5 m)
Trembleur - Pz7
hydraulic head threshold (102 m)
P1
Hasard-Cheratte Nord - Pz9
P3
Wandre - F5
F8
Hasard-Cheratte Sud - Pz8
Pz1
hydraulic head (m)
N
Meters
observed value
simulated value

Figure 6
Click here to download high resolution image

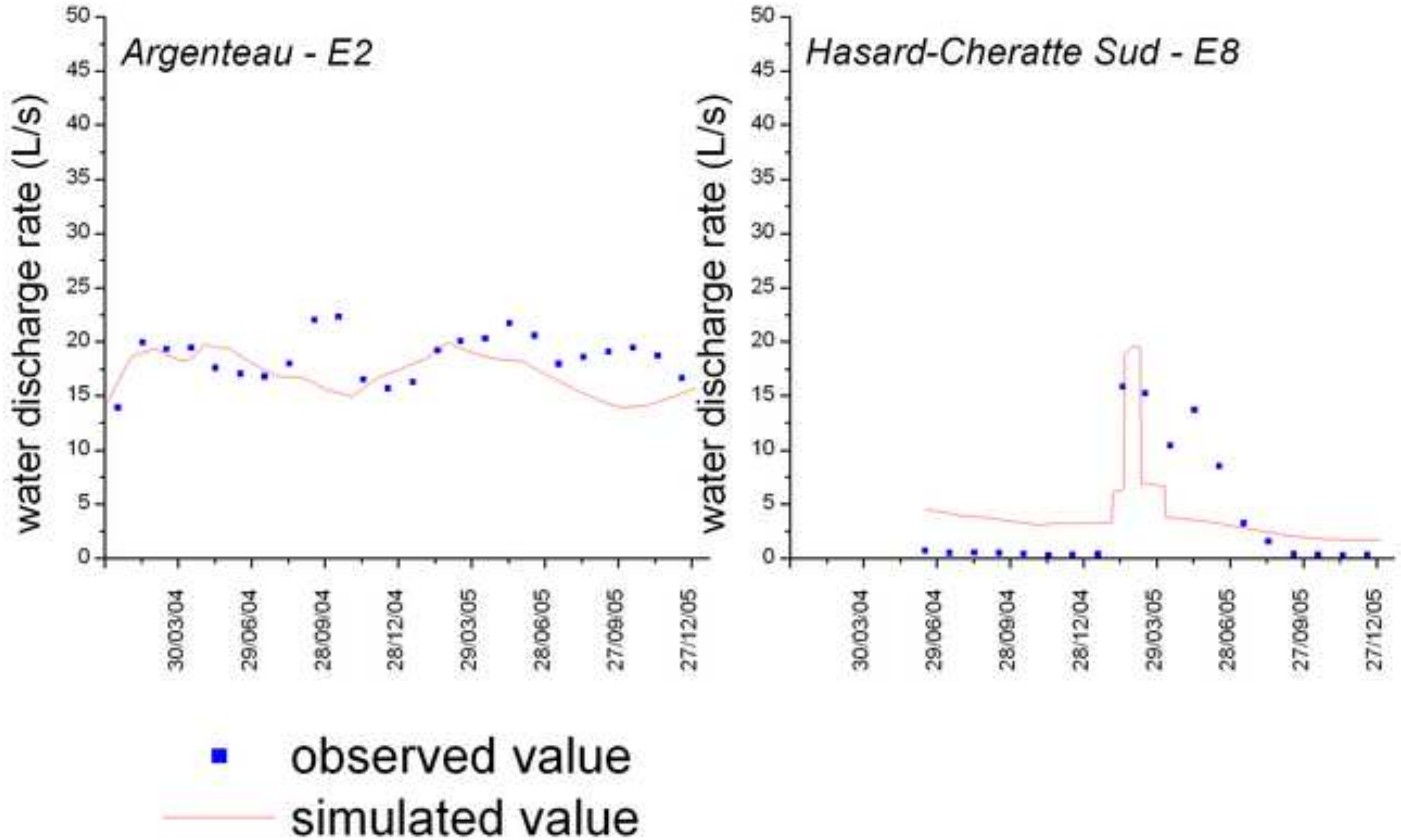

Figure 7
Click here to download high resolution image

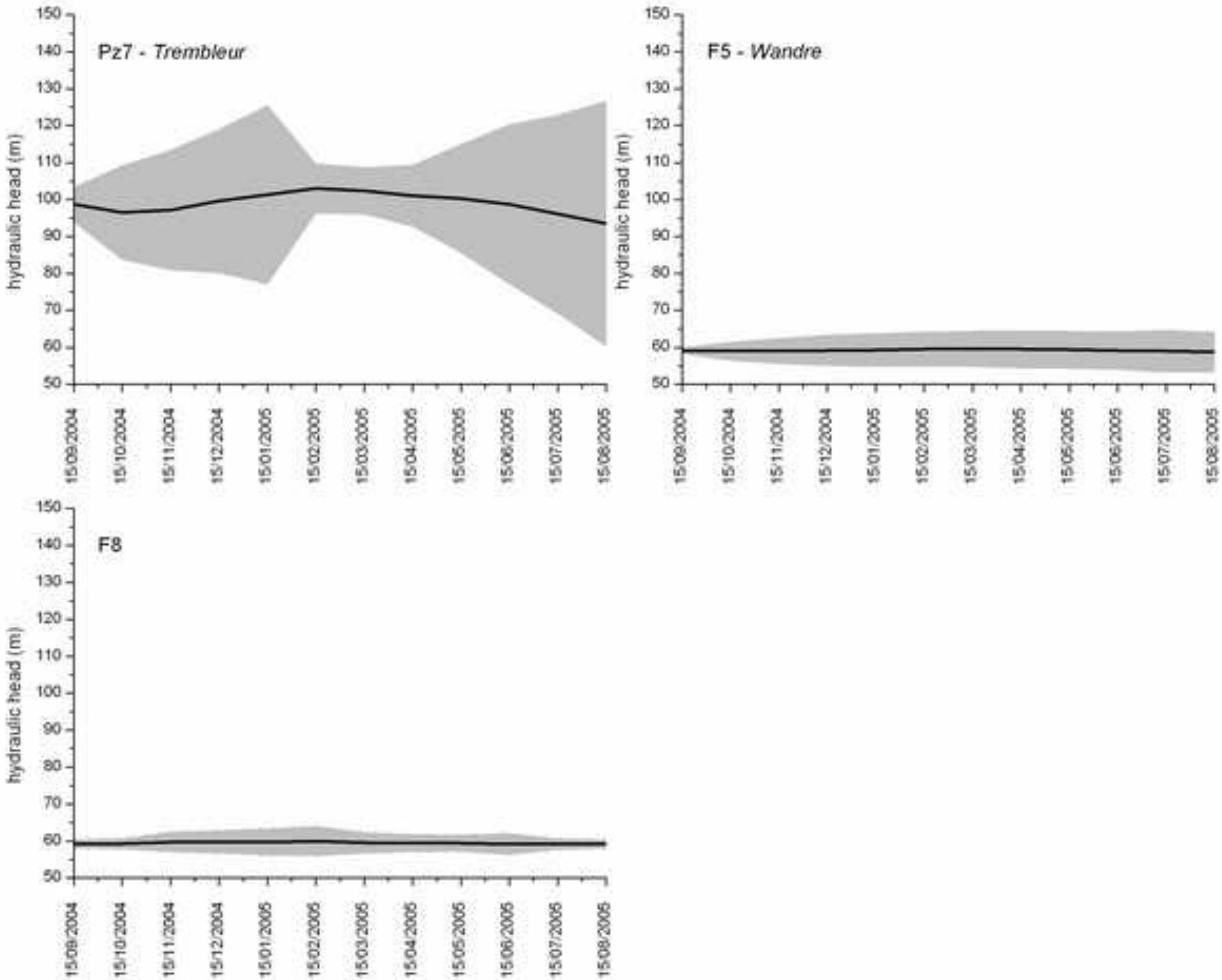

Figure 8
Click here to download high resolution image

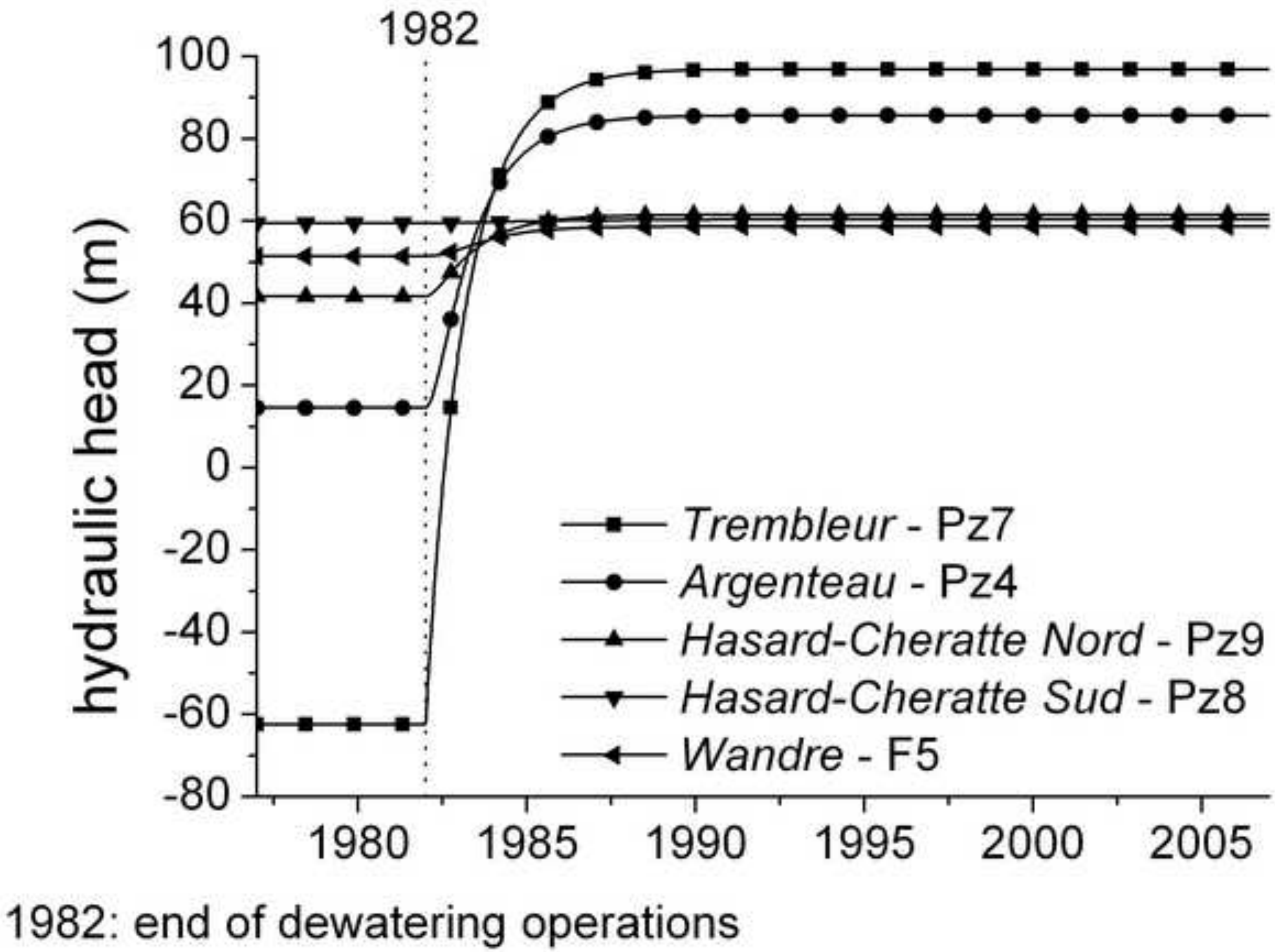

Figure 9
Click here to download high resolution image

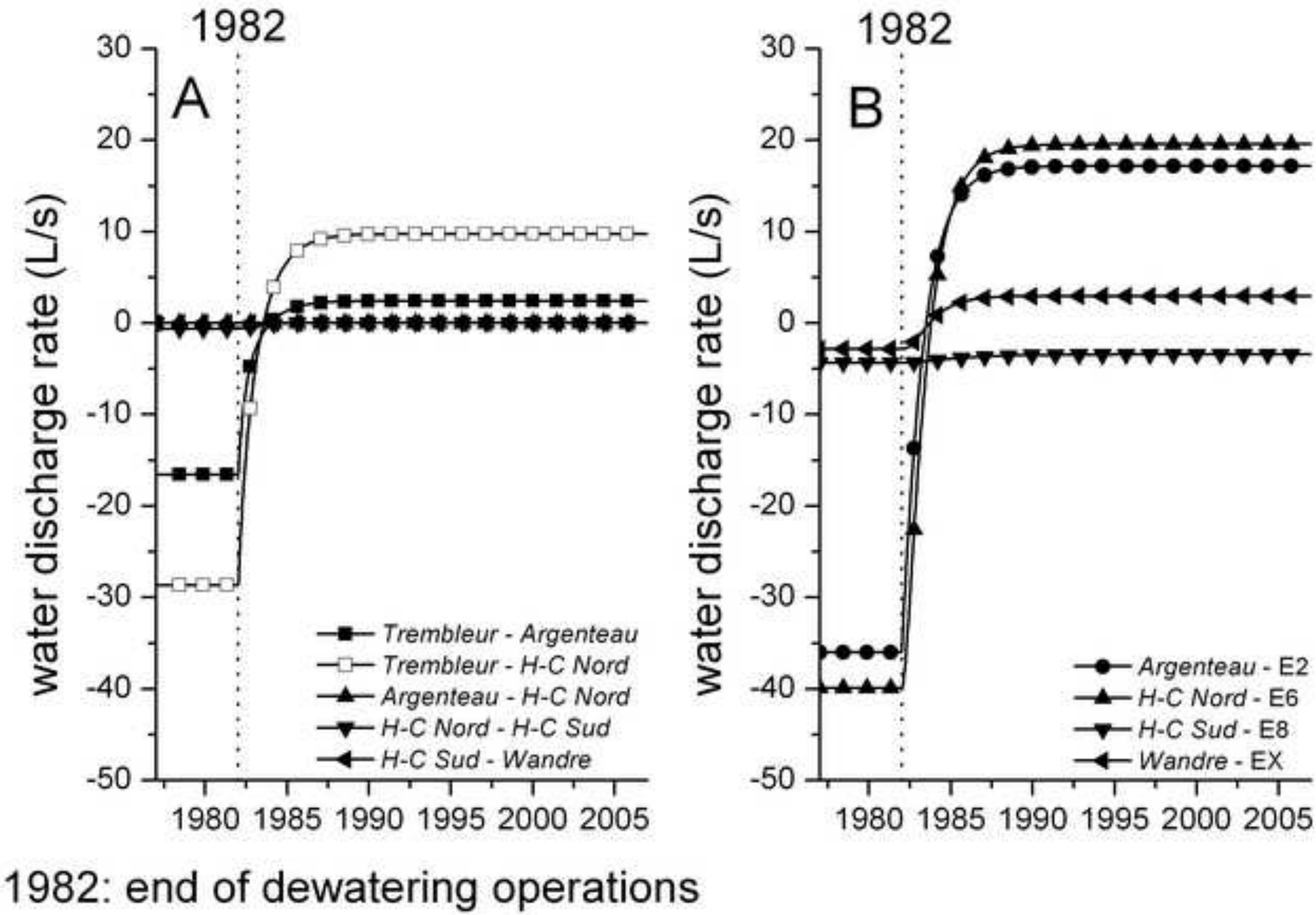

Figure 10

Click here to download high resolution image

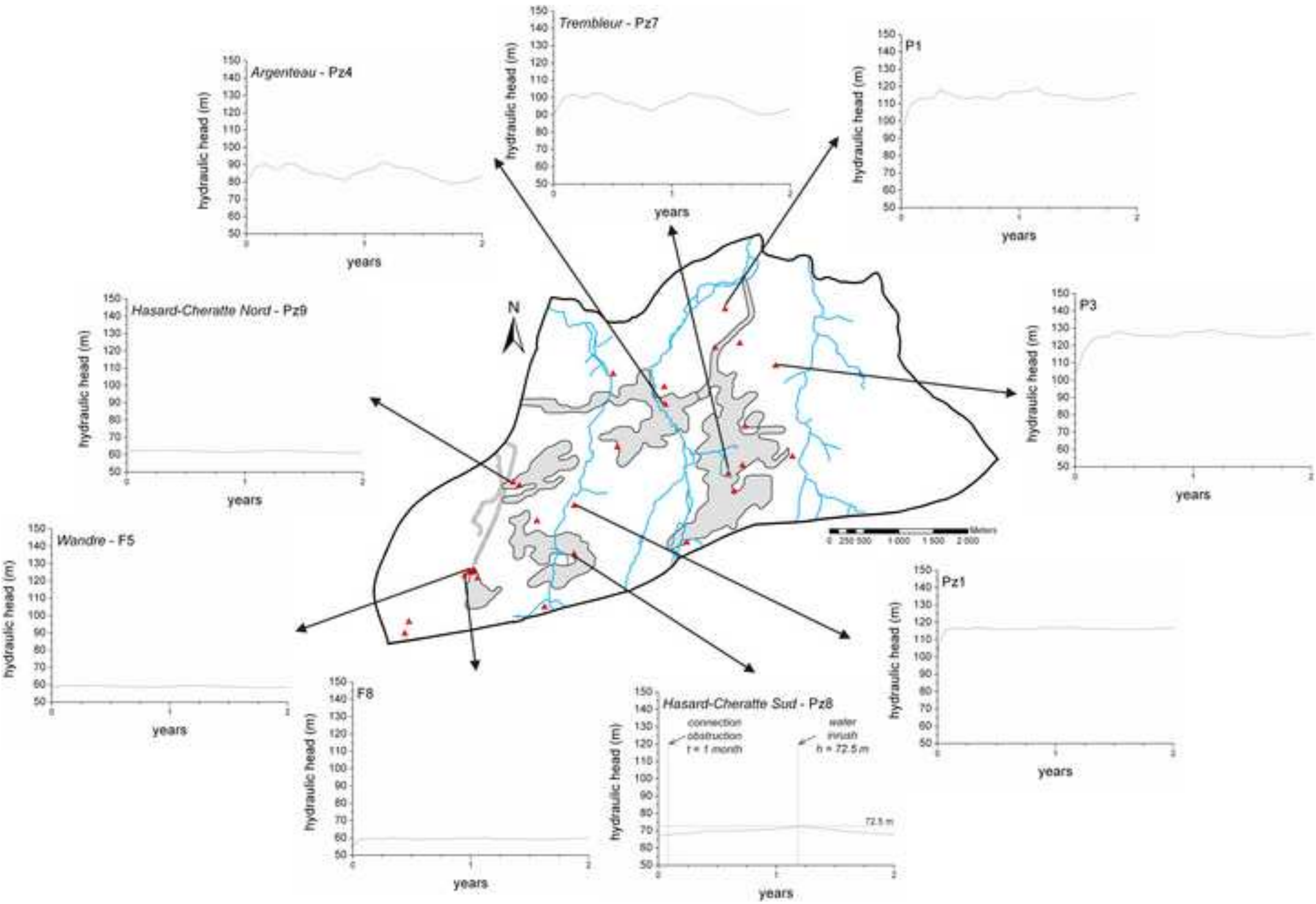

Figure 11

Click here to download high resolution image

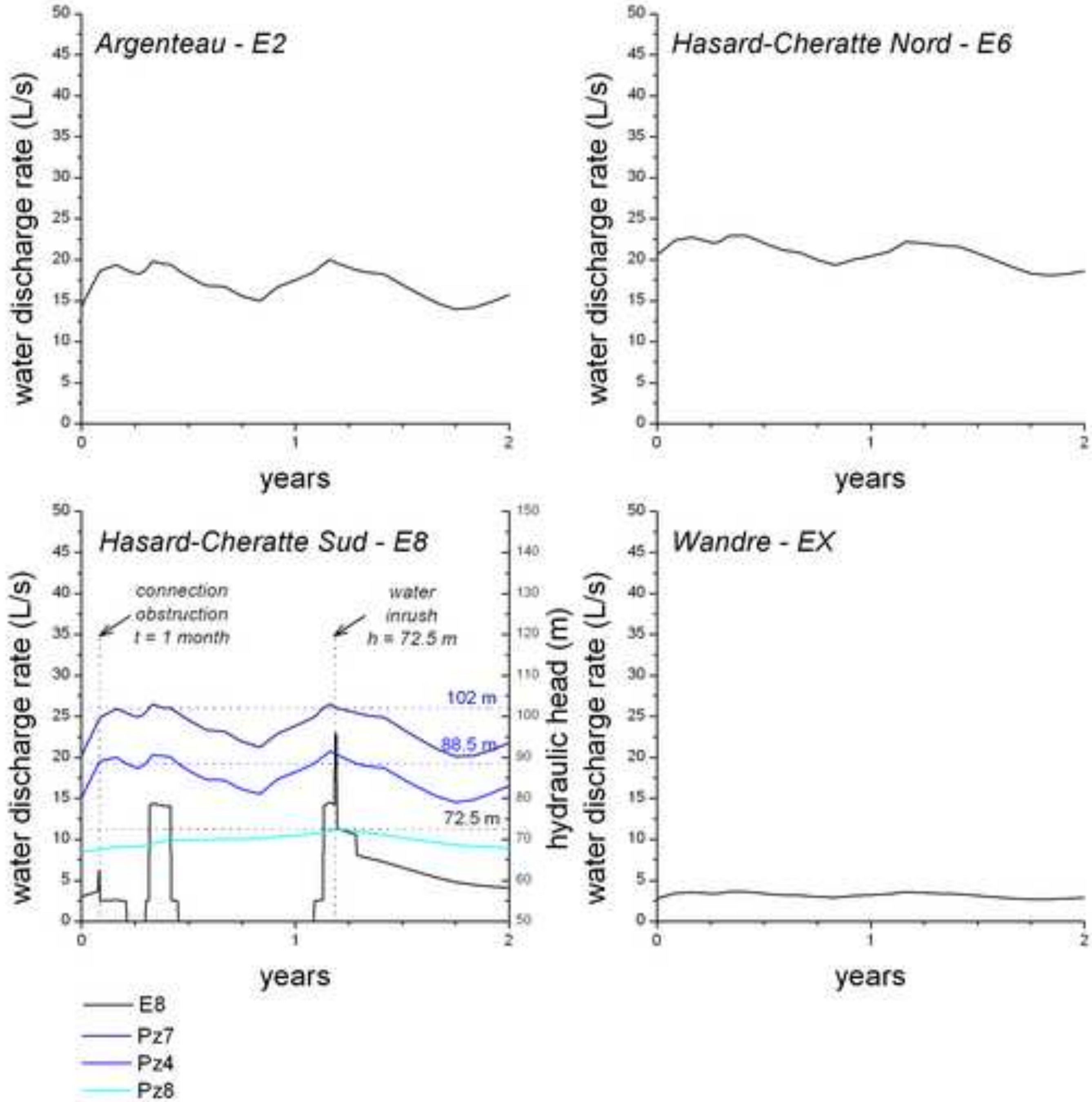

Figure 12
Click here to download high resolution image

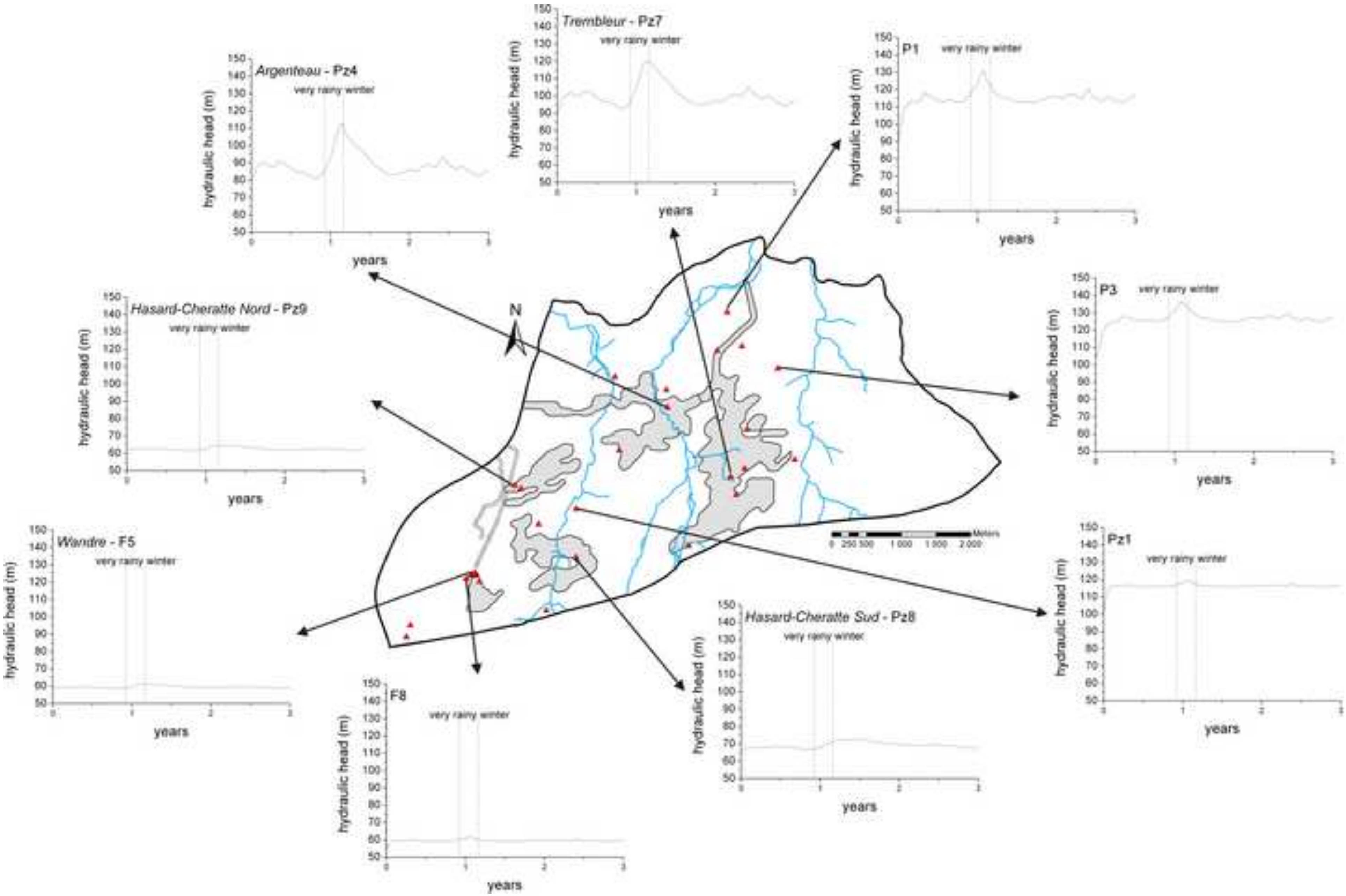

Figure 13
Click here to download high resolution image

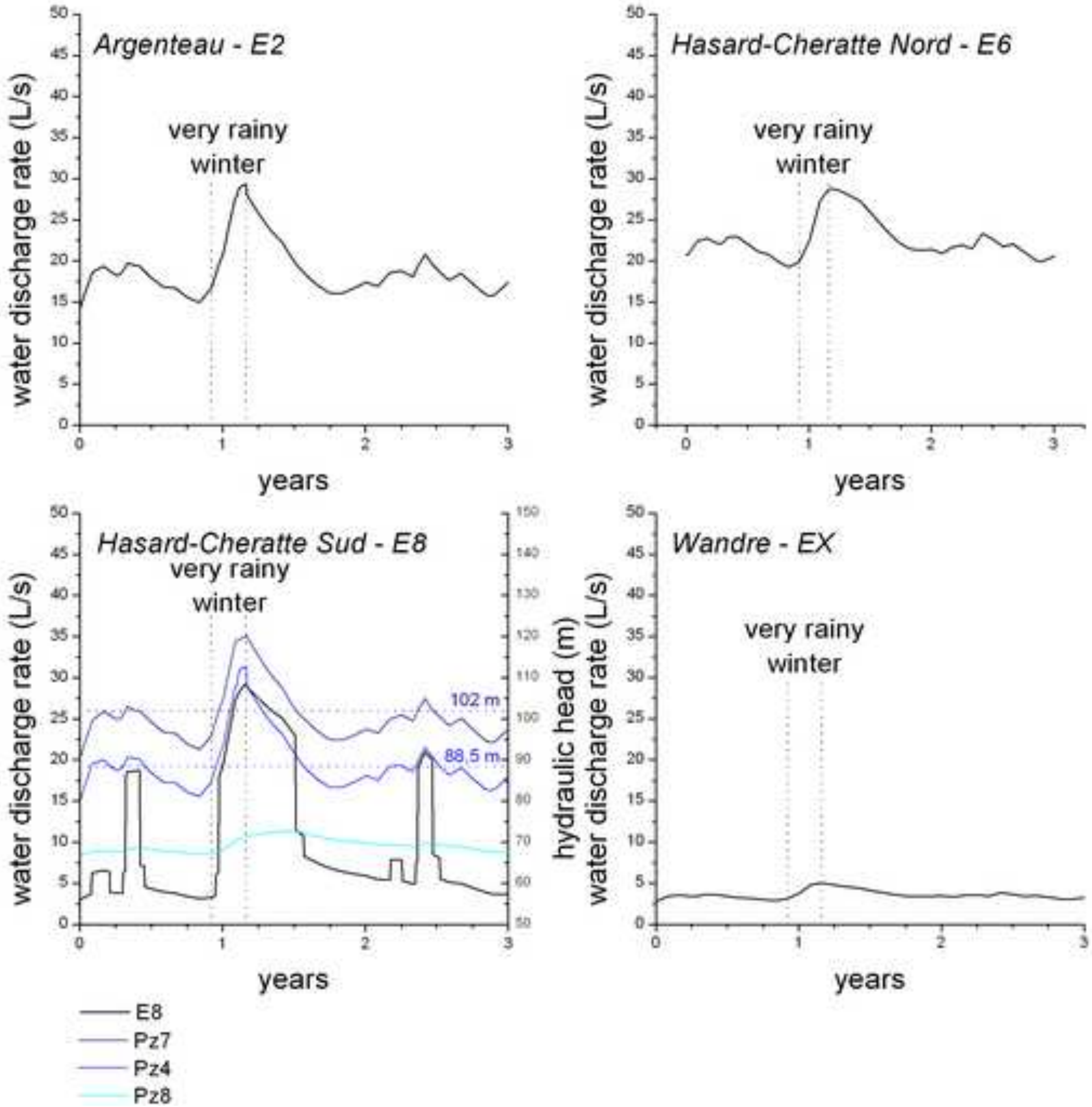

Table 1
Click here to download Table: Table_1.doc

	Parameters				
Geological formations	K (m/s)	S_y (-)	S_S (m^{-1})		
HOU	5.00×10^{-6}	0.10	1.00×10^{-4}		
VAA	3.00×10^{-6}	0.40	1.00×10^{-4}		
GUL	2.00×10^{-5}	0.05	1.00×10^{-4}		
ALA	7.00×10^{-5}	0.50	1.00×10^{-4}		
AMO	7.00×10^{-3}	0.50	1.00×10^{-4}		
Exploited zones		S_y (-)	S_S (m^{-1})		
Trembleur		0.006	1.00×10^{-6}		
Argenteau		0.006	1.00×10^{-6}		
Hasard-Cheratte Nord		0.07	1.00×10^{-6}		
Hasard-Cheratte Sud		0.07	1.00×10^{-6}		
Wandre		0.07	1.00×10^{-6}		
External BC				α (s^{-1})	H_{ref} (m)
Trembleur - Bolland R.				2.00×10^{-8}	92.00
Argenteau - Meuse R.				1.50×10^{-8}	55.00
collecting pipe 1 - Meuse R.				1.50×10^{-7}	55.00
collecting pipe 2 - Meuse R.				3.00×10^{-7}	55.00
unexploited zone - Meuse R.				5.00×10^{-5}	55.00
Internal BC				α (s^{-1})	
unexploited zone - exploited zones (vertical)				1.00×10^{-15}	
unexploited zone - exploited zones (horizontal)				1.00×10^{-12}	
By-pass flow connections				α (m^2/s)	
$\alpha_{Trembleur\text{-}Argenteau}$				2.15×10^{-4}	
$\alpha_{Trembleur\text{-}Hasard\text{-}Cheratte\ Nord}$				2.75×10^{-4}	
$\alpha_{Trembleur\text{-}Hasard\text{-}Cheratte\ Sud}$				3.00×10^{-4} if $h_{Trembleur}>102.0$ m	
$\alpha_{Argenteau\text{-}Hasard\text{-}Cheratte\ Nord}$				1.00×10^{-8}	
$\alpha_{Argenteau\text{-}Hasard\text{-}Cheratte\ Sud}$				1.00×10^{-4} if $h_{Argenteau}>88.5$ m	
$\alpha_{Hasard\text{-}Cheratte\ Nord\text{-}Hasard\text{-}Cheratte\ Sud}$				3.50×10^{-5}	
$\alpha_{Hasard\text{-}Cheratte\ Sud\text{-}Wandre}$				3.00×10^{-6}	
$\alpha_{Hasard\text{-}Cheratte\ Nord\text{-}collecting\ pipe\ 2}$				3.00×10^{-3}	
$\alpha_{Hasard\text{-}Cheratte\ Sud\text{-}collecting\ pipe\ 1}$				1.00×10^{-3}	
$\alpha_{Wandre\text{-}collecting\ pipe\ 2}$				8.00×10^{-4}	

K = hydraulic conductivity of the geological formations [LT^{-1}], S_y = specific yield (-), S_s = specific storage coefficient [L^{-1}], $\alpha_{i\text{-}j}$ = exchange coefficient for Fourier boundary conditions (external or internal) [T^{-1}] and by-pass flow connections [L^2T^{-1}], H_{ref} = drainage level [L]. Drainage levels have not been calibrated.

Table 2

Click here to download Table: Table_2_revised.doc

parameter	css
hydraulic conductivity of geological formations	
K	8.89×10^{-1}
specific yield of geological formations	
S_y	3.47
specific yield of exploited zones	
$S_{y,\ \mathit{Trembleur}}$	1.63
$S_{y,\ \mathit{Argenteau}}$	9.54×10^{-1}
$S_{y,\ \mathit{Hasard\text{-}Cheratte\ Nord}}$	1.63×10^{-1}
$S_{y,\ \mathit{Hasard\text{-}Cheratte\ Sud}}$	1.57×10^{-1}
$S_{y,\ \mathit{Wandre}}$	1.08×10^{-1}
exchange coefficient of external BC	
$\alpha_{\text{unexploited zone-Meuse R.}}$	1.54×10^{-1}
$\alpha_{\mathit{Argenteau}\text{-Meuse R.}}$	1.23
$\alpha_{\text{collecting pipe 1-Meuse R.}}$	1.57×10^{-1}
$\alpha_{\text{collecting pipe 2-Meuse R.}}$	1.57×10^{-1}
exchange coefficient of by-pass flow connections	
$\alpha_{\mathit{Trembleur\text{-}Argenteau}}$	2.93×10^{-1}
$\alpha_{\mathit{Trembleur\text{-}Hasard\text{-}Cheratte\ Nord}}$	7.71×10^{-1}
$\alpha_{\mathit{Trembleur\text{-}Hasard\text{-}Cheratte\ Sud}}$	0.00
$\alpha_{\mathit{Argenteau\text{-}Hasard\text{-}Cheratte\ Nord}}$	3.09×10^{-2}
$\alpha_{\mathit{Argenteau\text{-}Hasard\text{-}Cheratte\ Sud}}$	1.57×10^{-1}
$\alpha_{\mathit{Hasard\text{-}Cheratte\ Nord\text{-}Hasard\text{-}Cheratte\ Sud}}$	3.91×10^{-2}
$\alpha_{\mathit{Hasard\text{-}Cheratte\ Sud\text{-}Wandre}}$	1.98×10^{-1}
$\alpha_{\mathit{Hasard\text{-}Cheratte\ Nord}\text{-collecting pipe 2}}$	3.31×10^{-1}
$\alpha_{\mathit{Hasard\text{-}Cheratte\ Sud}\text{-collecting pipe 1}}$	1.37×10^{-1}
$\alpha_{\mathit{Wandre}\text{-collecting pipe 2}}$	1.04×10^{-1}